

Thermoelectric Properties of $\text{Bi}_2\text{Te}_3\text{-Sb}_2\text{Te}_3\text{-Sb}_2\text{Se}_3$ Pseudo-Ternary Alloys in the Temperature Range 77 to 300° K

W. M. YIM, E. V. FITZKE, F. D. ROSI
RCA Laboratories, David Sarnoff Research Center, Princeton, NJ, USA

Received 5 October 1965

The electrical resistivity, thermoelectric power and thermal conductivity of pseudo-ternary $\text{Bi}_2\text{Te}_3\text{-Sb}_2\text{Te}_3\text{-Sb}_2\text{Se}_3$ alloys were measured in the temperature range 77 to 300° K. From these measurements, figures of merit at various temperatures were calculated and compared with effective figures of merit obtained from the results of Peltier cooling. Best n-type figure of merit, 3.2×10^{-3} deg at 300° K, was found at the Bi_2Te_3 -rich region of the alloy system and the best room temperature p-type figure of merit, 3.4×10^{-3} deg, was obtained at the Sb_2Te_3 -rich end. Peltier couples constructed from these alloys reproducibly yielded a maximum cooling of 77.6° K from room temperature. The superior thermoelectric properties of these alloys were attributed to the reduction in the lattice thermal conductivity and its small temperature dependence, and the increase in the energy band gap of the alloys upon additions of Sb_2Se_3 .

1. Introduction

The early work of Ioffe [1] and of Goldsmid and Douglas [2] showed that the most promising material for the application of thermoelectricity to refrigeration was the compound semiconductor, Bi_2Te_3 . At the same time, the theoretical considerations of Ioffe *et al* [3] suggested that solid solution alloying could improve the thermoelectric figure of merit of semiconductors, where impurity scattering is predominant, by decreasing the lattice thermal conductivity without affecting the thermoelectric power and electrical resistivity. This concept led to considerable research in recent years on the thermoelectric properties of solid solution alloys of compound semiconductors and, in particular, those in the generalised system, $(\text{Bi,Sb})_2(\text{Te,Se})_3$. As a result, in the pseudo-binary system $\text{Sb}_2\text{Te}_3\text{-Bi}_2\text{Te}_3$, figures of merit in excess of $3 \times 10^{-3}/\text{deg}$ at room temperature have been reported for p-type alloys with alloy compositions ranging from 20 to 30 mole %

Bi_2Te_3 and doped with Se [4], excess Te [5], or both [6-9]. For n-type material, Bi_2Te_3 alloys containing 10 to 25 mole % Bi_2Se_3 doped with monovalent metal halides have been reported with room temperature figures of merit up to $2.8 \times 10^{-3}/\text{deg}$ [4], [10-12].

In a recent work on materials for thermoelectric refrigeration by Rosi, Abeles and Jensen [10], it was shown that the figure of merit (see section 2.2) for p-type $\text{Bi}_2\text{Te}_3\text{-20% Sb}_2\text{Te}_3$ * alloys was considerably improved by additions of as little as 5% Sb_2Se_3 in solid solution. This was analysed on the basis that the addition of Sb_2Se_3 raised the band gap of the alloys, which was considered necessary in order to avoid the deleterious effect of an overlap between the onset of degeneracy and an ambipolar contribution to the thermal conductivity due to the diffusion of electron-hole pairs [13]. It was further pointed out that p-type alloys in the vicinity of 30% $\text{Bi}_2\text{Te}_3\text{-70% Sb}_2\text{Te}_3$ would provide the highest figures of merit, since this

*All compositions are in mole %.

composition corresponds closely to the minimum in lattice thermal conductivity in this binary alloy system. Important in this connexion is the recent work of Smirous and Stourac [5], who reported a figure of merit as high as $3.58 \times 10^{-3}/\text{deg}$ for a 25% Bi₂Te₃ - 75% Sb₂Te₃ alloy containing 4 wt % excess Te.

In the present study, the earlier work of Rosi *et al* [10] was extended to include data on the thermoelectric properties of both n- and p-type Bi₂Te₃-Sb₂Te₃-Sb₂Se₃ pseudo-ternary alloy. The solid solution additions of the compound Sb₂Se₃ to Bi₂Te₃-Sb₂Te₃ alloys are of special interest for several reasons: firstly, Sb₂Se₃ has a higher band gap than either Bi₂Te₃ or Sb₂Te₃ (see table I); secondly, the crystal structure and average atomic mass of Sb₂Se₃ is different from that of Bi₂Te₃ or Sb₂Te₃, which may further enhance scattering of phonons due to random mass fluctuations and lattice strains; finally, Bi₂Te₃, Sb₂Te₃, and Sb₂Se₃ form solid solutions over a wide range of compositions except in the neighbourhood of large Sb₂Se₃ concentrations [18]. On the basis of exploratory data, the Sb₂Te₃ content was confined to 0 to 20% for n-type material, and 70 to 80% for p-type; the Sb₂Se₃ content in all cases was limited to 2 to 10%. The measurements of thermoelectric properties were extended to cover the temperature range, 77 to 300° K.

similar to that previously described [10], and at a rate of 0.6 cm/h and a temperature gradient of 25° C/cm near the solid-liquid interface [19]. The resulting ingots, 0.7 cm in diameter and 18 cm long, consisted of coarse grains whose cleavage characteristics suggested a strong preferred orientation with the {111} plane within 10° of the growth direction. A number of ingots were also prepared by the zone-levelling technique to improve the compositional homogeneity further. However, no significant difference was noted in the thermoelectric properties of these ingots as compared to those prepared by the Bridgman technique. This is understandable in view of the small separation between the liquidus and solidus curves in the Bi₂Te₃-Sb₂Te₃ phase diagram [20], which makes the solute distribution coefficient nearly equal to one. In addition, the distribution coefficient for Sb₂Te₃ in Bi₂Te₃ is larger than one, and in Sb₂Te₃ it is smaller than one. Thus, the distribution coefficient of the Sb₂Se₃ in the Bi₂Te₃-Sb₂Te₃ alloys would not be appreciably different from unity.

2.2. Measuring Techniques

Measurements of the thermal conductivity κ , thermoelectric power Q , and electrical resistivity ρ were made at room temperature and at a number of fixed points in the range 77 to 300° K. These provided a direct determination of the

TABLE I Crystal structure, average atomic mass and band gap of Bi₂Te₃, Sb₂Te₃ and Sb₂Se₃

Compound	Structure	Average atomic mass	Band gap (eV), 300° K	
			Thermal	Optical
Bi ₂ Te ₃	Rhombohedral	16.02	0.16 ^(a)	0.13 ^(b)
Sb ₂ Te ₃	Rhombohedral	125.3	0 ^(c)	0.3 ^(d)
Sb ₂ Se ₃	Orthorhombic	96.1		1.2 ^(d)

^(a): See reference 14

^(b): See reference 15

^(c): See reference 16, E_g derived from thermoelectric power measurements

^(d): See reference 17

2. Experimental Procedure

2.1. Preparation of Alloys

In the preparation of the pseudo-ternary Bi₂Te₃-Sb₂Te₃-Sb₂Se₃ alloys, a high purity grade (99.999%) of the component elements was used; and these were obtained from the American Smelting and Refining Company. The alloys were grown by a vertical Bridgman technique

material's *figure of merit*, $z = Q^2/\rho\kappa$. These properties were measured with specimens in the form of short cylinders with temperature gradient or electrical current applied in the direction of the axis of the cylinder. As a result of the preferred crystal growth, this direction was nearly perpendicular to the <111> axis of the crystallites.

The room temperature thermal conductivity

was measured by the standard method of placing the sample between a heater and heat sink; a detailed sketch of the apparatus was given in a previous work [10]. The apparatus was checked using a fused quartz standard, which has a κ similar to the Bi_2Te_3 alloys at 300° K. In addition, the temperature dependence of κ for fused quartz is well defined [21, 22]. The thermoelectric power was determined simultaneously with κ by measuring the Seebeck voltage across the specimen with copper branches of the heater and heat sink thermocouples. The room temperature electrical resistivity was determined by a resistance scanner with a Keithley AC milliohm-meter. The voltage probes consisted of one fixed lead attached to one end of the specimen and one potential probe which was moved along the length of the specimen by a motor drive. Resistance as a function of distance between the probes was recorded on a strip chart; and from the slope of the plot and the known dimensions of the sample, the resistivity was calculated. The use of the resistance scanner also provided a means of checking the homogeneity of the alloy ingots, since any inhomogeneity resulted in nonlinear resistance-distance profiles. In all cases, 80% of the ingot gave a uniform value of resistivity.

The temperature variations of κ and Q were measured in the range, 77 to 300° K, using a specially constructed apparatus. The apparatus is, in principle, similar to the one used in the measurements of the room temperature properties except that the entire apparatus can be immersed into various coolants. To reduce thermal contact resistance, the sample was soldered with an indium-gallium eutectic alloy (24.5% In by weight, freezing point $\sim 16^\circ\text{C}$, $\rho_{300^\circ\text{K}} \sim 3 \times 10^{-5} \Omega\text{cm}$, and $\rho_{77^\circ\text{K}} \sim 5 \times 10^{-6} \Omega\text{cm}$) between the heater and heat sink. The temperature dependence of ρ was measured with the Keithley milliohmmeter at various fixed temperatures. In some cases, an x - y recorder was used to obtain resistance-temperature plots while the specimen was allowed to warm up slowly from 77° K. The resistivities calculated from both methods were in excellent agreement. The reproducibility of all measurements on a single specimen was $\pm 0.5\%$ for Q and ρ , and $\pm 1\%$ for κ .

Hall coefficient measurements at room temperature and 77° K were made on single crystal specimens, approximately $7 \times 2 \times 0.3$ mm, which were cleaved from the bulk materials. A

magnetic field was applied perpendicular to the cleavage plane and a current was passed in a direction parallel to the cleavage plane. In order to eliminate thermoelectric and thermomagnetic effects and the potential differences arising from any slight misalignment of probes, the Hall voltage was determined as an average of four measurements with opposite directions of magnetic field and opposite directions of current. The electrical resistivity was an average of two measurements with the current in opposite directions. The difference between room temperature values of ρ measured on the Hall specimens and those obtained from the resistance scanning of the ingot was less than $\pm 5\%$. The reproducibility of the Hall coefficient on a single specimen was $\pm 3\%$ at room temperature and $\pm 0.6\%$ at liquid nitrogen temperature.

After the measurements of individual properties, Peltier cooling couples were constructed from a selected group of p- and n-type alloys. The dimensions of couple legs were optimised to give a maximum coefficient of performance in accordance with the expression

$$\left(\frac{l}{A}\right)_p \left(\frac{A}{l}\right)_n = \left[\left(\frac{\kappa}{\rho}\right)_p \left(\frac{\rho}{\kappa}\right)_n\right]^{1/2}$$

where A is the cross-sectional area and l is the length of the couple legs; the subscripts p and n denote the p- and n-legs, respectively. Under this condition, the figure of merit of the couple, Z_{cal} , calculated from the direct measurements of ρ , Q , and κ of each leg can be shown as

$$Z_{\text{cal}} = \frac{(Q_p - Q_n)^2}{[(\sqrt{\rho\kappa})_p + (\sqrt{\rho\kappa})_n]^2}$$

The peltier cooling was measured in a vacuum of 10^{-4} mm Hg and at various hot junction temperatures from 77 to 300° K. From the measured values of maximum Peltier cooling, ΔT_{max} , the effective figures of merit of the couple, Z_{eff} , were obtained by using the relationship

$$Z_{\text{eff}} = 2 \Delta T_{\text{max}} / T_c^2$$

where T_c is the cold junction temperature. This relationship is valid only when the materials properties are temperature independent; but it is a good approximation, if the temperature difference between the hot and cold junctions is small. The direct measurements of Z_{eff} provided an independent means of checking the accuracy of the measurements of individual materials properties.

2.3. Calculation of Transport Parameters

The lattice thermal conductivity, carrier concentration, mobility, and effective mass were calculated from the results of the temperature dependence of thermoelectric properties and the Hall measurements.

The lattice thermal conductivity, κ_{ph} , was obtained from the measured total thermal conductivity, κ , by using the simple relation

$$\kappa = \kappa_{ph} + \kappa_{el},$$

which assumes no ambipolar contribution, κ_{amb} . The electronic contribution, κ_{el} , was calculated from the Weidemann-Franz relation

$$\kappa_{el} = L_0 \sigma T,$$

where

$$L_0 = L'_0 \left(\frac{k}{e} \right)^2$$

is the Lorentz number, and

$$L'_0 = \frac{1}{(kT)^2} \left[\frac{K_3}{K_1} - \left(\frac{K_2}{K_1} \right)^2 \right]$$

and

$$K_n = \frac{2^{3/2} m^{*1/2}}{3\pi^2 \hbar^3} \int_0^\infty \tau(E) E^{n+1/2} \frac{\partial f_0(\eta^*)}{\partial E} dE$$

$$\left. \begin{array}{l} m^* = \text{effective mass} \\ \tau = \text{relaxation time} \\ E = \text{kinetic energy} \\ f_0 = \text{Fermi distribution function} \\ \eta^* = \text{reduced Fermi level} \end{array} \right\} \text{of charge carriers}$$

The problem here is to evaluate the Lorentz number, which must be related to the Fermi level. Amith [23], in his recent study of the semiconductor transport phenomena for mixed scattering and arbitrary degeneracy, has presented his results in convenient graphical forms. Using these graphs, L_0 was calculated by estimating η^* from the measured values of thermoelectric power and assuming lattice scattering.

In an extrinsic semiconductor the Hall coefficient, R_H , is related to the carrier concentration, n , by

$$R_H = \frac{Ar}{ne}$$

where A and r are the constants which depend on the band structure, scattering mechanism and degree of degeneracy. For spherical bands, A is equal to one; but for highly oblate energy surfaces, such as those in Bi₂Te₃, the value A can be much smaller [24, 25]. Since no direct

determination of the band structures of the Bi₂Te₃ alloys has been made, a value of one was assumed for A ; and r values were estimated from the results of Amith [23]. The Hall mobility μ was determined from the relation

$$\mu = R_H \sigma$$

where σ is the electrical conductivity.

The effective mass m^* was calculated from the following equation (assuming again the spherical band structure):

$$n = \frac{4}{\sqrt{\pi}} \left(\frac{2\pi m^* kT}{h^2} \right)^{3/2} F_{1/2}(\eta^*)$$

or more conveniently,

$$\left(\frac{m^*}{m_0} \right)^{3/2} = \frac{n}{\left[2.85 \times 10^{19} \left(\frac{T}{300} \right)^{3/2} \right] F_{1/2}(\eta^*)}$$

where m_0 is the mass of a free electron and F is the Fermi integral. It must be remembered that the effective mass entering into the calculation of transport properties for many valley semiconductors, such as Bi₂Te₃ and its alloys, is the density-of-states effective mass. However, the effective mass calculated as above with the assumption of spherical band is still a useful parameter to estimate the relative magnitude of the quantity, $(\mu/\kappa_{ph}) (m^*/m_0)^{3/2}$, which is proportional to the figure of merit, as will be discussed in the section to follow.

3. Results and Discussion

3.1. Undoped Pseudo-Ternary Alloys

The pseudo-ternary alloys, Bi₂Te₃-Sb₂Te₃-Sb₂Se₃, without impurity additions always exhibited p-type conductivity. The room temperature electrical resistivity, thermoelectric power, and thermal conductivity of these undoped alloys as a function of composition are given in fig. 1. The Sb₂Se₃ concentration in the undoped alloys was held at a constant level of 5 mole %, which is well within the solid solubility limit as revealed by metallographic examinations. It is seen that with increasing amount of Sb₂Te₃ both ρ and Q decrease, while κ_{ph} shows a broad minimum of about 0.8×10^{-2} W/cm deg between 50 to 70 mole % Sb₂Te₂. The minimum lattice thermal conductivity of the pseudo-ternary alloys, $0.8_0 \times 10^{-2}$ W/cm deg, is larger than that of 0.5×10^{-2} W/cm deg reported by Rosi *et al* [10] for the pseudo-binary Bi₂Te₃-Sb₂Te₃ alloys at about 65% Sb₂Te₃, but somewhat lower than the 0.9×10^{-2} W/cm deg value

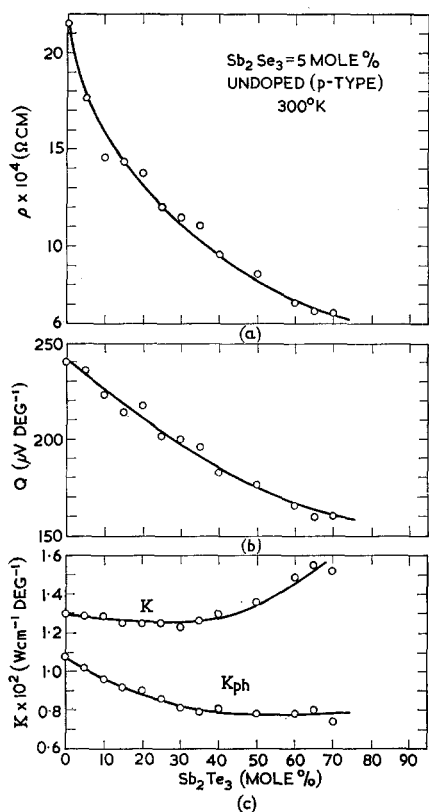


Figure 1 Dependence of electrical resistivity (ρ), thermoelectric power (Q), and thermal conductivity (κ) on composition in undoped Bi_2Te_3 - Sb_2Te_3 - Sb_2Se_3 alloys at 300°K .

obtained by Goldsmid [26]. It must be remembered, however, that the alloys used by Rosi *et al* to determine κ_{ph} were heavily doped with Bi to insure complete degeneracy. Important in this connexion is the recent work of Beers *et al* [27] and Steigmeier and Abeles [28] who showed that scattering of phonons by charge carriers is an important mechanism responsible for a decrease in κ_{ph} of heavily doped Ge and Ge-Si alloys. It is likely, therefore, that the lower value of κ_{ph} obtained by Rosi *et al* is a result of the additional contribution of phonon-charge carrier scattering.

The Hall coefficient, carrier concentration and Hall mobility data are presented in fig. 2. The Hall coefficients at 300°K are larger than those at 77°K at all compositions, but the difference becomes smaller as the Sb_2Te_3 concentration increases. The trend seems to be related to a

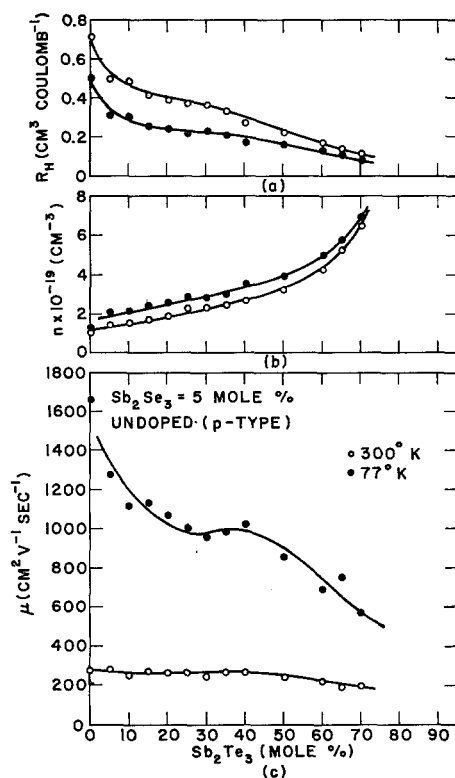


Figure 2 Dependence of Hall coefficient (R_H), carrier concentration (n), and Hall mobility (μ) on composition in undoped Bi_2Te_3 - Sb_2Te_3 - Sb_2Se_3 alloys at 77 and 300°K .

change in the degree of degeneracy with temperature; however, the difference is too large to be accounted for in this way. It is unlikely that the difference is due to a change in the scattering mechanism or in the band structure over the indicated temperature range. Some temperature variations of the Hall coefficient in Bi_2Te_3 have been reported previously, but no satisfactory explanation has yet been offered [24, 29]. The difference in the Hall coefficients between 300°K and 77°K is reflected on the calculated carrier concentrations; but as seen in fig. 2, the Hall mobilities are much more temperature-dependent than the carrier concentrations. This would suggest that the temperature variation of the electrical resistivity is mostly due to changes in the mobility with temperature.

It is noteworthy that the thermoelectric powers of the pseudo-ternary Bi_2Te_3 - Sb_2Te_3 - Sb_2Se_3 alloys are larger than those of the pseudo-binary Bi_2Te_3 - Sb_2Te_3 alloys [30] for similar carrier concentrations[†]. This would indicate that the

[†]The carrier concentrations n of the Bi_2Te_3 - Sb_2Te_3 alloys were recalculated from the original R_H values given in reference [30], using the same statistics as that used to calculate n of the Bi_2Te_3 - Sb_2Te_3 - Sb_2Se_3 alloys.

density-of-states effective mass for the pseudo-ternary alloys is larger. In addition, a larger value of m^* makes it possible to accommodate a higher carrier concentration without encountering degeneracy and an accompanying decrease in thermoelectric power.

It has been shown from transport theory that the figure of merit of an extrinsic semiconductor is related to the density-of-states effective mass m^* , the carrier mobility μ , and the lattice thermal conductivity κ_{ph} , by the expression [1]

$$z \propto \left(\frac{\mu}{\kappa_{ph}} \right) \cdot \left(\frac{m^*}{m_0} \right)^{3/2}$$

In fig. 3, it may be seen that for the undoped pseudo-ternary alloys the quantity $(\mu/\kappa_{ph})(m^*/m_0)^{3/2}$ shows three prominent peaks as a function of Sb₂Te₃ content: a small one at 5 mole %, an intermediate one at 25 mole %, the largest at 70 mole % Sb₂Te₃. Consequently, alloys of these compositions containing suitable doping agents were investigated most extensively with a view toward obtaining both n- and p-type materials with high figures of merit.

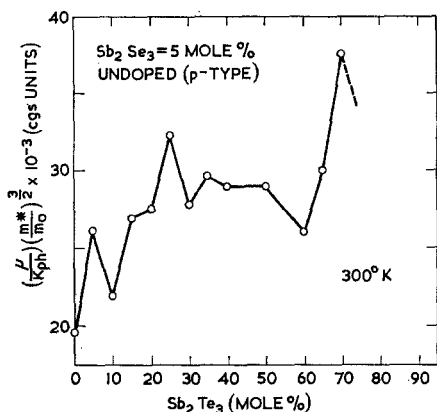


Figure 3 Dependence of $(\mu/\kappa_{ph})(m^*/m_0)^{3/2}$ on composition in undoped Bi₂Te₃-Sb₂Te₃-Sb₂Se₃ alloys at 300° K.

3.2. Doped Pseudo-Ternary Alloys at 300° K

3.2.1. n-type Alloys at 300° K

Since the undoped pseudo-ternary alloys were p-type, suitable impurity additions were required to convert them to n-type semiconductors. Halides of Cu and Ag have been widely used as donor impurities in Bi₂Te₃ and its alloys; however, it is now known that they are not suitable because of the fast diffusion rate of Cu or Ag ions even at room temperature [31, 32].

Our observations on the CuI- or AgI-doped alloys showed darkening of the ingot surface on standing at room temperature, due evidently to oxidation of Cu or Ag diffusing to the surface. The loss of the metal ions from solid solution would result in depletion of donor concentrations and subsequent increase in the electrical resistivity of the alloys. Indeed, our results showed a two-fold increase in ρ of these alloys after storage for a year. The fast diffusion of Cu or Ag ions can be rationalised on the basis of an interstitial diffusion mechanism. The Cu or Ag would go into and move through the interstitial positions between two adjacent layers of electronegative atoms (Te₁-Te₁) in the host alloy lattice, where the interatomic spacing is largest and the binding force weakest [33]. This consideration clearly points to the need for doping materials which are soluble substitutionally in the host alloy. Among those investigated, SbI₃ was found to be most suitable, because it exhibited a considerable solubility in the pseudo-ternary alloys (up to 0.2 wt %) and the SbI₃-doped alloys showed no resistivity deterioration over long periods of time at room temperature. Based on the carrier concentrations calculated from the Hall measurements and the impurity concentrations as determined from chemical analysis, SbI₃ was found to give 4.4 electrons/mole, a value similar to that reported for SbCl₃ (4.5 electrons/mole) [11].

The Bi₂Te₃-rich pseudo-ternary alloys, when doped with SbI₃ to provide optimum ρ , gave the best n-type figures of merit. The Sb₂Te₃-rich alloys, in spite of their lower κ_{ph} , did not provide good n-type material. These alloys showed n-type conductivity only upon impurity additions beyond the solid solubility limit, as indicated by the presence of precipitates and a high degree of polycrystallinity. The strong p-type characteristics of the Sb₂Te₃-rich alloys is analogous to that of pure Sb₂Te₃ on which attempts to change its conductivity from p- to n-type have not been successful.

The thermoelectric properties at room temperature of the best n-type alloy, (Bi₂Te₃)₉₀(Sb₂Te₃)₅(Sb₂Se₃)₅ doped with SbI₃, are shown in fig. 4. This alloy with a ρ of about $10 \times 10^{-4} \Omega \text{ cm}$ has provided a z of $3.2 \times 10^{-3}/\text{deg}$, the best value reported to date for n-type material. Small variations in the major composition, Sb₂Te₃ ranging from 0 to 5 mole % and Sb₂Se₃ ranging from 5 to 2 mole %, also gave z values higher than $3 \times 10^{-3}/\text{deg}$.

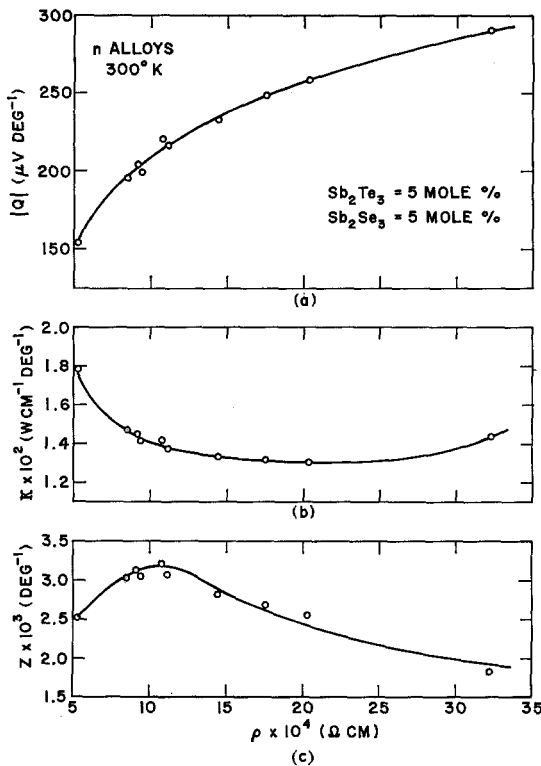


Figure 4 Dependence of thermoelectric power (Q), thermal conductivity (κ), and figure of merit (z) on electrical resistivity (ρ) in n-type $(\text{Bi}_2\text{Te}_3)_{90}(\text{Sb}_2\text{Te}_3)_5(\text{Sb}_2\text{Se}_3)_5$ alloys at 300° K.

The total thermal conductivity decreased with increasing resistivity (fig. 4b) as one would expect from the consideration of the electronic contribution to the thermal conductivity, which is inversely proportional to ρ . However, beyond a ρ of about 25×10^{-4} Ω cm, the κ is seen to rise slightly. This is more clearly shown in fig. 5, where κ is plotted against σ . The increase in κ can be attributed to an ambipolar contribution arising from the diffusion of electron-hole pairs down the temperature gradient with the onset of intrinsic conduction [13]. To avoid this deleterious effect, materials have to be doped down well below the intrinsic resistivity. However, with materials of low band gap this degree of doping results in degeneracy and, consequently, lowering of the figure of merit. The requirement of large band gap with respect to κT , therefore, is obvious. In the pseudo-ternary alloys, the ambipolar contribution at room temperature would be very small below the intrinsic resistivity of 25×10^{-4} Ω cm, and can certainly be neglected in the optimum resistivity range of 9×10^{-4} to 12×10^{-4} Ω cm.

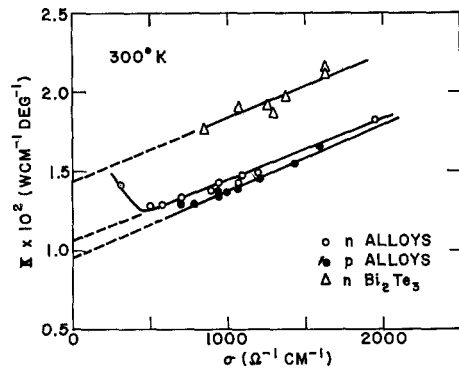


Figure 5 Dependence of thermal conductivity (κ) on electrical conductivity (σ) in n-type $(\text{Bi}_2\text{Te}_3)_{90}(\text{Sb}_2\text{Te}_3)_5(\text{Sb}_2\text{Se}_3)_5$, p-type $(\text{Sb}_2\text{Te}_3)_{72}(\text{Bi}_2\text{Te}_3)_{25}(\text{Sb}_2\text{Se}_3)_3$ alloys, and n-type Bi_2Te_3 at 300° K.

The slope of the linear portion of the plot in fig. 5 gave a value of 1.8 for the scattering factor L' , which compares favourably with a calculated value of 2.1. For a non-degenerate electron gas with lattice scattering, theory predicts a value of 2.0. Therefore, the assumption of lattice scattering made in calculating the Lorentz number is a reasonable one. The intercept at zero σ gave a lattice thermal conductivity of about 1.0×10^{-2} W/cm deg for the n-type $(\text{Bi}_2\text{Te}_3)_{90}(\text{Sb}_2\text{Te}_3)_5(\text{Sb}_2\text{Te}_3)_5$ alloys. This lattice thermal conductivity, κ_{ph} , is lower than that of a pseudo-binary Bi_2Te_3 -10% Sb_2Te_3 alloy (1.2×10^{-2} W/cm deg) [10]; and is still lower by almost 40% than that of SbI_3 -doped Bi_2Te_3 . Although some dependence of κ_{ph} on the carrier concentration or on σ has been reported previously [34], the linear extrapolation method of determining κ_{ph} in the range of σ studied here is justified, for L'_0 was found to be a slowly varying function of σ .

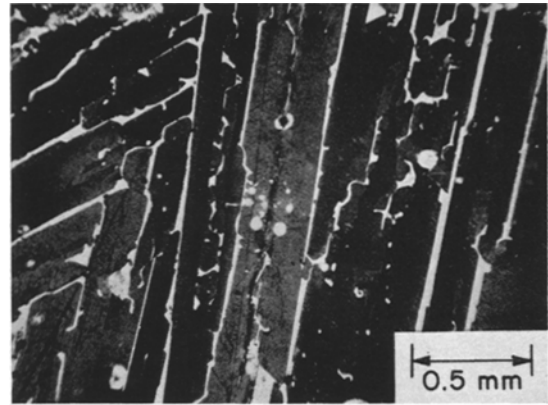
3.2.2. p-type Alloys at 300° K

In view of the largest value of $(\mu/\kappa_{ph})(m^*/m_0)^{3/2}$ (see fig. 3) near 70% Sb_2Te_3 , it is expected that this composition may yield the best p-type alloys. This indeed was the case. The Bi_2Te_3 -rich alloys, on the other hand, did not provide good p-type material. Since the electrical resistivities of the undoped Bi_2Te_3 -rich alloys were high, attempts were made to dope these alloys to the optimum ρ ($\sim 10 \times 10^{-4}$ Ω cm) by additions of acceptor impurities, such as Pb and Ge. However, the highest z value found in the Bi_2Te_3 -rich end was only 2.8×10^{-3} /deg at about 20% Sb_2Te_3 .

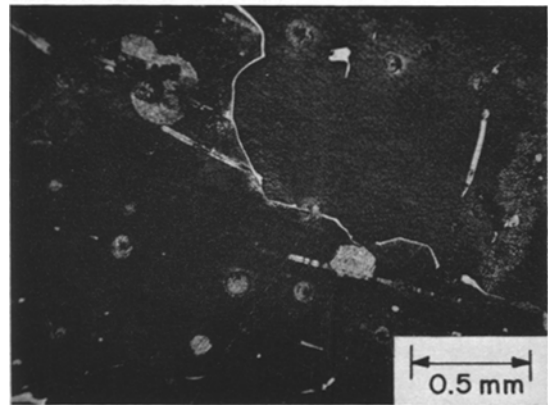
For the Sb₂Te₃-rich alloys near 70% Sb₂Te₃, it was necessary to raise the resistivity by compensation because the ρ of these alloys ($\sim 6 \times 10^{-4} \Omega \text{ cm}$) was too low for an optimum z . Results on doping with SbI₃ showed that ρ could be increased to $8.5 \times 10^{-4} \Omega \text{ cm}$, but beyond this range intrinsic conduction set in as evidenced by a drop in Q and an increase in κ . Subsequently, the resistivity of these alloys was increased to the optimum value by additions of excess Te or Se, which were found previously to be suitable dopants for the pseudo-binary Sb₂Te₃-25% Bi₂Te₃ alloys [4-9]. It has been pointed out by Rosi *et al* [4] that the addition of Se in these pseudo-binary alloys, unlike excess Te, should result in preferential formation of selenides, which have higher free energy of formation than the tellurides of Bi or Sb [35]. Hence, the alloys containing Se are actually pseudo-ternary solid solutions of Sb₂Te₃-Bi₂Te₃-Sb₂Se₃ with excess Te. This realisation led to the selection of Te as the dopant for the p-type Sb₂Te₃-rich ternary alloys.

The solid solubility of Te in these alloys is estimated to be less than 0.2 at. % by metallographic examination. The excess Te precipitates out as a second phase along grain boundaries and cleavage planes. This is shown in the photomicrograph of fig. 6a for a Te-doped (Sb₂Te₃)₇₂(Bi₂Te₃)₂₅(Sb₂Se₃)₃, where the second phase precipitates appear as white platlets. The results of electron microprobe analysis showed that the second phase consisted mainly of Te with small amounts of Bi, Sb and Se. The way in which this Te-rich second phase distributed itself in the matrix alloy was found to have a marked effect on the thermoelectric properties. Thus, alloys containing continuous platlets (fig. 6a) showed lower z values than those with random distribution of discrete particles of the second phase (fig. 6b). This, in turn, was found to be related to the alloy growth parameters, details of which will be presented in another paper [19].

The thermoelectric properties of the Te-compensated (Sb₂Te₃)₇₂(Bi₂Te₃)₂₅(Sb₂Se₃)₃ alloys are shown in fig. 7. A maximum z value of $3.4 \times 10^{-3}/\text{deg}$ is obtained at a ρ of $10.7 \times 10^{-4} \Omega \text{ cm}$. Alloys having compositions of Sb₂Te₃ ranging from 70 to 72 mole %, Sb₂Se₃ from 5 to 3 mole %, and excess Te from 2 to 5 wt % all provided z values higher than $3.0 \times 10^{-3}/\text{deg}$. The lattice thermal conductivity of the Te-doped (Sb₂Te₃)₇₂(Bi₂Te₃)₂₅(Sb₂Se₃)₃ alloys



(a)



(b)

Figure 6 Te-rich second phase in p-type (Sb₂Te₃)₇₂-(Bi₂Te₃)₂₅(Sb₂Se₃)₃ alloys. Etchant = 1 HNO₃ : 2 HCl : 2 sat. K₂S₂O₈ in H₂O (a) Growth rate = 7.6 cm/h $z_{300^\circ\text{K}} = 2.3 \times 10^{-3}/\text{deg}$; (b) Growth rate = 0.6 cm/h $z_{300^\circ\text{K}} = 3.4 \times 10^{-3}/\text{deg}$.

obtained from fig. 5 is $0.96 \times 10^{-2} \text{ W/cm deg}$. This value is probably higher than the true κ_{ph} for single-phase alloys of similar composition, because the Te-rich second phase present in the alloys is known to enhance the thermal conduction by "circulating currents" [36, 37]. Therefore, the true κ_{ph} , referring to the undoped alloys of similar composition (fig. 1c), is estimated to have a value of about $0.8 \times 10^{-2} \text{ W/cm deg}$. The high values of z for the present n- and p-type pseudo-ternary alloys have undoubtedly resulted from the decrease in κ_{ph} on alloying; however, with increasing alloy additions of Sb₂Se₃ the carrier mobility decreases to such a point that the reduction in κ_{ph} no

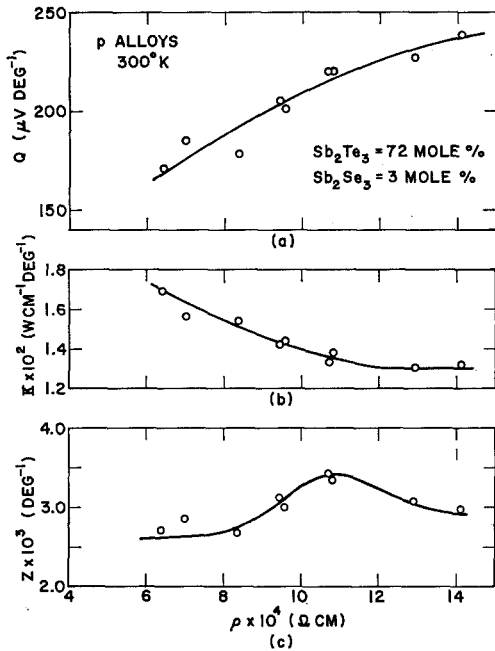


Figure 7 Dependence of thermoelectric power (Q), thermal conductivity (κ), and figure of merit (z) on electrical resistivity (ρ) in p-type $(\text{Sb}_2\text{Te}_3)_{72}(\text{Bi}_2\text{Te}_3)_{25}(\text{Sb}_2\text{Se}_3)_3$ alloys at 300°K .

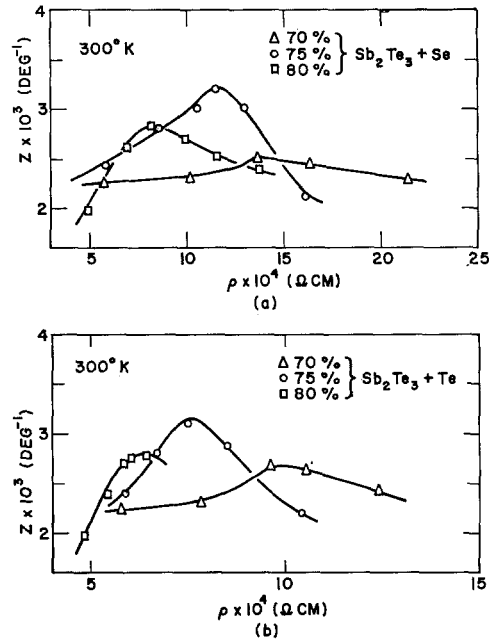


Figure 8 Dependence of figure of merit (z) on electrical resistivity (ρ) in p-type $\text{Sb}_2\text{Te}_3\text{-Bi}_2\text{Te}_3$ alloys doped with Se and Te at 300°K .

longer brings about higher z . This was the case for all alloys containing more than 5 mole % Sb_2Se_3 .

Since the composition of the pseudo-ternary alloys near 70% Sb_2Te_3 containing excess Te is similar to that of the pseudo-binary $\text{Sb}_2\text{Te}_3\text{-}25\%$ Bi_2Te_3 alloys doped with excess Se or excess of both Se and Te, it would be interesting to compare their thermoelectric properties. In figs. 8a and 8b are presented thermoelectric figures of merit of the Se-doped and Te-doped pseudo-binary alloys in the range of Sb_2Te_3 content from 70 to 80 mole %. In both cases, metallographic examinations revealed the presence of a second phase, whose compositions were found to be similar ($\sim 90\%$ Te by electron microprobe analysis). It is also interesting to note that during differential thermal analysis, the second phase, whether it resulted from the excess additions of Se, Te, or S, melted at approximately the same temperature ($\sim 415^\circ\text{C}$), indicating that the second phase consisted mainly of a eutectic, rich in Te (melting point $T_e = 452^\circ\text{C}$). These observations confirm the earlier assumption of Rosi *et al* [4] on the preferential formation of selenides of high free energy of formation with additions of excess selenium.

The thermoelectric properties of the Se-doped $\text{Sb}_2\text{Te}_3\text{-}25\%$ Bi_2Te_3 (fig. 8a) are seen to be similar to those of the Te-doped $(\text{Sb}_2\text{Te}_3)_{72}(\text{Bi}_2\text{Te}_3)_{25}(\text{Sb}_2\text{Se}_3)_3$, although for the latter alloy the maximum z is slightly higher (3.4×10^{-3} as compared to $3.2 \times 10^{-3}/\text{deg}$ in the former). This can be attributed to minor differences in the alloy composition or to the distribution of the Te-rich second phase.

Two important features in figs. 8a and 8b should be noted. First, in both cases the maximum z is shifted toward lower ρ with increasing Sb_2Te_3 content in the major alloy composition. Second, in a given host alloy composition, the maximum z for the Se-doped alloys occurred at higher ρ than that for the Te-doped alloys. From these results it would appear that the band gap of the alloys decreased with increasing Sb_2Te_3 , as reported by Rosi [10], and increased with additions of Se presumably through the formation of Sb_2Se_3 in solid solution.

3.3. Temperature Dependence of Thermoelectric Properties of Doped Pseudo-Ternary Alloys

The temperature dependence of ρ , Q , and κ_{ph} for the n- and p-type pseudo-ternary $\text{Bi}_2\text{Te}_3\text{-}$

Sb₂Te₃-Sb₂Se₃ alloys with carrier concentrations ranging from 1.5×10^{19} to about $7 \times 10^{19}/\text{cm}^3$ are shown in figs. 9 to 11. The electrical resistivity of the best n-type ($n = 3.6 \times 10^{19}/\text{cm}^3$) and p-type alloys ($n = 2.1 \times 10^{19}/\text{cm}^3$) varied as $T^{1.2}$ and $T^{1.6}$, respectively, in the range 150 to 300° K (see fig. 9). Over the same temperature range, the temperature exponent decreased with increasing carrier concentrations; namely, for n-type alloys it varied from 1.3 to 0.9, and for the p-type alloys from 1.8 to 1.4. Below 150° K, the temperature dependence was less steep, but it deviated from a simple power law. It was mentioned earlier that the temperature variation of ρ for the ternary alloys, as in Bi₂Te₃ [24, 25, 38], was due primarily to the change of mobility with temperature. For non-degenerate semiconductors with acoustic lattice scattering, the mobility is expected to vary as $T^{-1.5}$. Hence, the resistivity should vary as $T^{1.5}$, and would approach $T^{1.0}$ with increasing degeneracy. Since this is consistent with the observed temperature dependence of ρ , it would appear that lattice scattering is the dominant scattering mechanism in the ternary alloys. For comparison, in Bi₂Te₃ the reported values of the temperature exponent are 1.68 for n-type [25] and 1.98 for p-type [24].

Fig. 10 shows a linear variation of thermoelectric power with $\ln T$ over the temperature range, 150 to 300° K. Goldsmid [38] showed that the thermoelectric power of a non-degenerate extrinsic semiconductor having spherical

or ellipsoidal band should vary linearly with $\ln T$ in a temperature range where the carrier concentration remains constant. The plot of Q against $\ln T$, according to the theory, should consist of parallel lines each having a slope equal to $3/2 (k/e)$ or $129 \mu\text{V}/\text{deg}$. This compares favourably with the experimental values of 110 and $155 \mu\text{V}/\text{deg}$ for the n- and p-type pseudo-ternary alloys, respectively, since such factors as a rise in the density-of-states effective mass with temperature, a warped energy surface, and a change in the energy dependence of relaxation time can affect these values. It is also seen from fig. 10 that the Q of the n-type alloys shows a weaker temperature dependence than that of the p-type. Further, the temperature dependence becomes less steep as the carrier concentration increases in a manner similar to the resistivity variation with the carrier concentration.

While the temperature dependence of ρ and Q of the ternary alloys is generally similar to that of Bi₂Te₃, there is a marked difference in the temperature dependence of the lattice thermal conductivity between the two materials, as shown in fig. 11. From 300 to about 200° K, there is only a small increase in the κ_{ph} of the ternary alloys with temperature; but, in the range between 150 to 77° K, κ_{ph} varies as $T^{-0.7}$ for the n-type alloys and as $T^{-0.6}$ for the p-type alloys. For comparison, κ_{ph} for n-type Bi₂Te₃ shows a $T^{-1.2}$ dependence, which is similar to the usual T^{-1} behaviour associated with the lattice scattering.

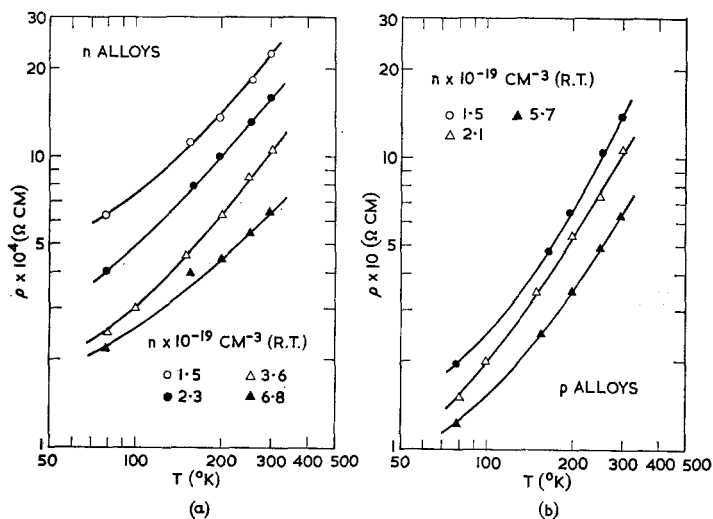


Figure 9 Temperature dependence of electrical resistivity (ρ) in n-type $(\text{Bi}_2\text{Te}_3)_{93}(\text{Sb}_2\text{Te}_3)_5(\text{Sb}_2\text{Se}_3)_2$ and p-type $(\text{Sb}_2\text{Te}_3)_{72}(\text{Bi}_2\text{Te}_3)_{25}(\text{Sb}_2\text{Se}_3)_3$ alloys.

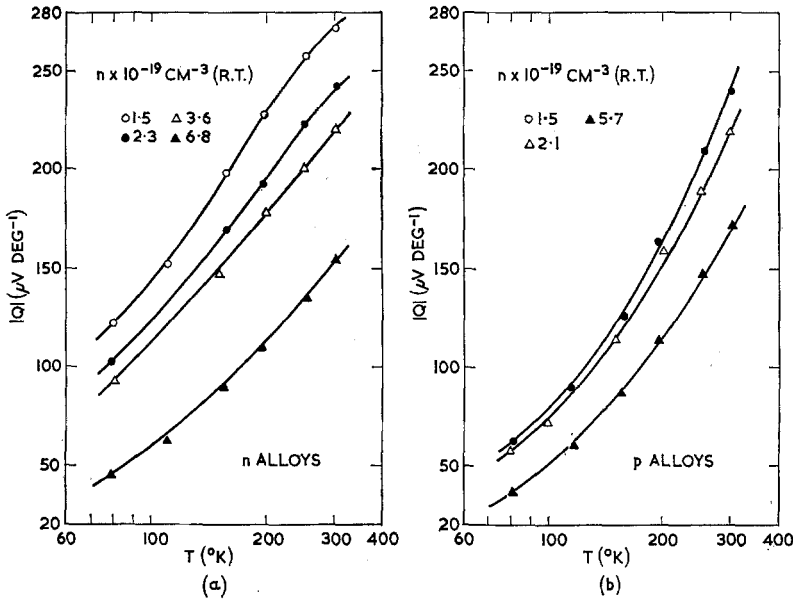


Figure 10 Temperature dependence of thermoelectric power (Q) in n-type $(\text{Bi}_2\text{Te}_3)_{90}(\text{Sb}_2\text{Te}_3)_5(\text{Sb}_2\text{Se}_3)_5$ and p-type $(\text{Sb}_2\text{Te}_3)_{72}(\text{Bi}_2\text{Te}_3)_{25}(\text{Sb}_2\text{Se}_3)_3$ alloys.

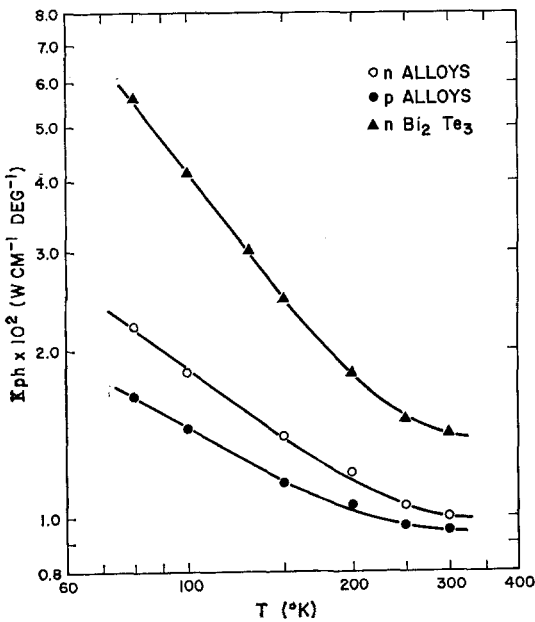


Figure 11 Temperature dependence of lattice thermal conductivity (κ_{ph}) in n-type $(\text{Bi}_2\text{Te}_3)_{90}(\text{Sb}_2\text{Te}_3)_5(\text{Sb}_2\text{Se}_3)_5$, p-type $(\text{Sb}_2\text{Te}_3)_{72}(\text{Bi}_2\text{Te}_3)_{25}(\text{Sb}_2\text{Se}_3)_3$ alloys, and n-type Bi_2Te_3 .

merit to vary only slightly in this range. Below 200°K however, z decreases rapidly due mainly to a steep rise in κ_{ph} . This is shown in fig. 12, where z of the n- and p-type pseudo-ternary alloys are presented as a function of temperature. It is noteworthy that the z maxima appear to shift in the direction of lower temperatures with decreasing carrier concentrations. According to the earlier theory by Ioffe [1], the optimum carrier concentration, n_{opt} , to provide maximum z has the following form:

$$n_{opt} \propto \frac{2(2\pi m^* \kappa T)^{3/2}}{h^3}$$

This assumes lattice scattering, and that both the lattice thermal conductivity and carrier mobility are invariant with carrier concentration. The observed temperature variation of n_{opt} however, departs appreciably from the predicted $T^{3/2}$ behaviour. Furthermore, in the temperature range studied, an alloy with the highest z at room temperature also exhibits a higher z at all other temperatures below 300°K . Thus, for cooling applications, it is essential to select the ternary alloy which is doped to give the highest z value at room temperature.

3.4 Some Pseudo-Ternary Alloys Containing Sulfides

The improvement of z by the solid-solution

Since the electrical resistivity, thermoelectric power, and lattice thermal conductivity show very little temperature variation over the range 200 to 300°K , one would expect the figure of

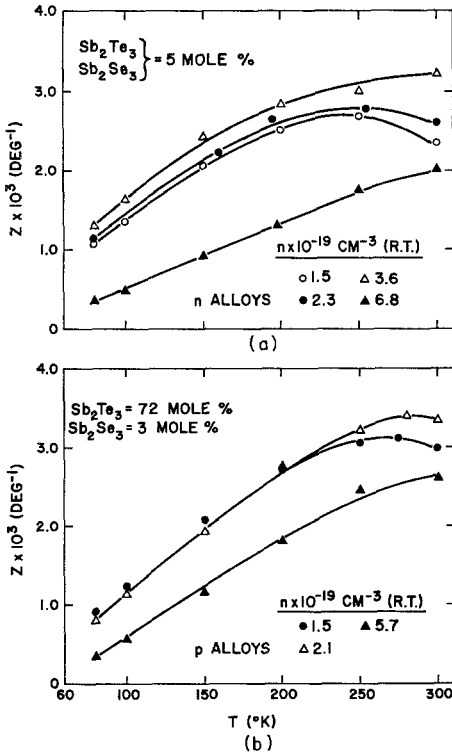


Figure 12 Temperature dependence of figure of merit (z) in n-type $(\text{Bi}_2\text{Te}_3)_{90}(\text{Sb}_2\text{Te}_3)_5(\text{Sb}_2\text{Se}_3)_5$ and p-type $(\text{Sb}_2\text{Te}_3)_{72}(\text{Bi}_2\text{Te}_3)_{25}(\text{Sb}_2\text{Se}_3)_3$ alloys.

additions of Sb_2Se_3 to the Bi_2Te_3 - Sb_2Te_3 alloys suggested that other alloying additions might also be beneficial. Although the results were not favourable, a brief discussion is in order. One of the compounds selected was Bi_2S_3 because it has a high band gap, 1.3 eV, and it is soluble up to a few mole % in Bi_2Te_3 [39]. Further, Airapetiants *et al* [40] reported that the electron mobility was practically unchanged on alloying Bi_2Te_3 with up to 30 mole % Bi_2S_3 . This implies that the ratio (μ/κ_{ph}) would increase on alloying with Bi_2S_3 .

In all cases the Bi_2S_3 additions were limited up to 5 mole %, and the alloys were doped n-type with SbI_3 . The room temperature thermoelectric properties of the n-type Bi_2Te_3 - Sb_2Te_3 - Bi_2S_3 alloys at the Bi_2Te_3 -rich region showed that κ_{ph} of the Bi_2S_3 alloys ($0.9 \times 10^{-2} \text{ W/cm deg}$) was slightly lower than that of Sb_2Se_3 alloys ($1.0 \times 10^{-2} \text{ W/cm deg}$). However, the ratio Q^2/ρ was inferior: $3.3 \times 10^{-5} \text{ W/cm deg}$ as compared to $4.5 \times 10^{-5} \text{ W/cm deg}$ for the Sb_2Se_3 alloys. This would suggest that the electron mobility or the product, $\mu(m^*/m_0)^{3/2}$,

was substantially reduced on alloying with Bi_2S_3 , contrary to the data of Airapetiants *et al* [40]. In addition, the sulfide additions resulted in brittle ingots.

Other ternary alloys studied were n-type Bi_2Te_3 - Bi_2Se_3 - Bi_2S_3 , p-type Sb_2Te_3 - Bi_2Te_3 - Bi_2S_3 and Sb_2Te_3 - Bi_2Te_3 - Sb_2S_3 . Their thermoelectric figures of merit were, however, much inferior to the ternary alloys containing Sb_2Se_3 .

3.5. Peltier Cooling

Peltier cooling measurements were made with thermocouples constructed from the best ternary alloy compositions. Typical results are shown in fig. 13 as a function of hot junction temperature. The carrier concentrations were $3.6 \times 10^{19}/\text{cm}^3$ and $2.1 \times 10^{19}/\text{cm}^3$ at room temperature for the n- and p-type branches, respectively. The temperature dependence of z for these branch compositions were given by the curves connecting open

Figure 13 Peltier cooling as a function of electrical current at various hot junction temperatures for Bi_2Te_3 - Sb_2Te_3 - Sb_2Se_3 alloy couple.

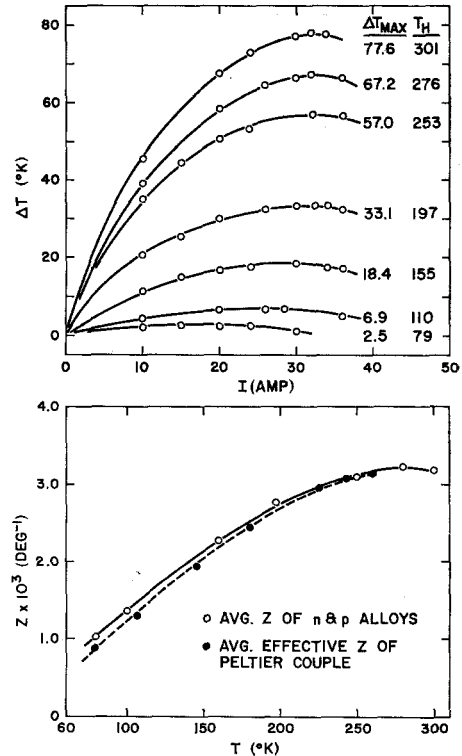


Figure 14 Comparison of average Z_{cal} with average Z_{eff} at various temperatures for Bi_2Te_3 - Sb_2Te_3 - Sb_2Se_3 alloy couple.

triangles in fig. 12. It is noteworthy that these Peltier couples have reproducibly provided a maximum cooling ΔT_{\max} from room temperature of 77.6° K, the highest value reported to date. As expected from thermodynamic efficiency considerations and in view of the decrease in z with temperature, the ΔT_{\max} decreased with hot junction temperature.

In fig. 14, the thermocouple figure of merit calculated from the direct measurements of ρ , Q , and κ at various temperatures for each branch, Z_{cal} , is compared with the effective figure of merit, Z_{eff} , obtained from the cooling measurements. The Z_{eff} of the couple is plotted at a mean temperature, which is defined as $1/2(T_h + T_c)$. It is seen that the Z_{cal} and the Z_{eff} are in excellent agreement in the range from 230 to 300° K. Below this temperature range, the Z_{eff} falls slightly below the Z_{cal} , but the agreement is still good.

The good agreement between Z_{cal} and Z_{eff} indicates a high degree of reliability in the measurements of the individual parameters. Furthermore, the maximum Peltier cooling of 77.6° K from room temperature shows the usefulness of the Bi_2Te_3 - Sb_2Te_3 - Sb_2Se_3 pseudo-ternary alloys as practical cooling materials. Indeed, a ΔT_{\max} as high as 141° K from 300° K has recently been achieved by a six-stage Peltier cooler constructed from these pseudo-ternary alloy thermoelements [41].

4. Conclusions

The pseudo-ternary Bi_2Te_3 - Sb_2Te_3 - Sb_2Se_3 system yields thermoelectric cooling materials which are superior to any pseudo-binary alloys. Their superiority is attributed to the low lattice thermal conductivity and its small temperature dependence. While the temperature dependence of thermoelectric power and electric resistivity of the ternary alloys indicates that lattice scattering is the dominant mode of scattering, the lattice thermal conductivity shows much less temperature variation than predicted by the theory. The experimental results also indicate that the high figures of merit of these solid-solution alloys can be attributed to the increase in the energy band gap of the Bi_2Te_3 - Sb_2Te_3 alloys with additions of Sb_2Se_3 . This prevents an overlap between degeneracy and the ambipolar contribution to the thermal conductivity on achieving optimum carrier concentrations through impurity additions.

It has been determined that SbI_3 is the most

stable dopant for the Bi_2Te_3 -rich n-type ternary alloys, and that excess Te is the most suitable dopant for the Sb_2Te_3 -rich p-type ternary alloys. The n-type $(\text{Bi}_2\text{Te}_3)_{90}(\text{Sb}_2\text{Te}_3)_5(\text{Sb}_2\text{Se}_3)_5$ alloy provided a figure of merit of $3.2 \times 10^{-3}/\text{deg}$ at 300° K, while the p-type $(\text{Sb}_2\text{Te}_3)_{72}(\text{Bi}_2\text{Te}_3)_{25}(\text{Sb}_2\text{Se}_3)_3$ alloy gave a room temperature figure of merit of $3.4 \times 10^{-3}/\text{deg}$. These alloys, as branches of a thermocouple circuit, have reproducibly yielded a maximum Peltier cooling of 77.6° K from a hot junction temperature of 300° K. Furthermore, a temperature as low as 159° K has recently been attained from room temperature by a six-stage Peltier cooler constructed from these ternary alloys.

Acknowledgements

The authors are grateful to Messrs T. V. Pruss and E. J. Stofko for their assistance in the experimental work. Acknowledgements are also due to Drs E. F. Hockings and A. Amith for helpful discussions.

References

1. A. F. IOFFE, "Semiconductor thermoelements and thermoelectric cooling" (Infosearch Ltd, London, 1957).
2. H. J. GOLDSMID and R. W. DOUGLAS, *Brit. J. Appl. Phys.* **5** (1954) 386.
3. A. F. IOFFE, S. V. AIRAPETIANTS, A. V. IOFFE, N. V. KOLOMOETS, and L. S. STIL'BANS, *Dokl. Akad. Nauk. SSSR* **106** (1956) 981.
4. F. D. ROSI, E. F. HOCKINGS, and N. E. LINDENBLAD, *RCA Rev.* **22** (1961) 82.
5. K. SMIROUS and L. STOURAC, *Z. Naturf.* **14a** (1959) 848.
6. J. B. CONN, E. J. SHEEHAN, and R. C. TAYLOR, *Adv. Energy Conv.* **1** (1961) 119.
7. J. RUPPRECHT, *Z. Naturf.* **17a** (1962) 628.
8. P. BERGVALL and O. BECKMAN, *Solid-State Electr.* **6** (1963) 133.
9. G. GRAMBERG and H. G. PLUST, *Helv. Phys. Acta* **36** (1963) 237.
10. F. D. ROSI, B. ABELES, and R. V. JENSEN, *J. Phys. Chem. Solids* **10** (1959) 191.
11. G. N. GORDIAKOVA, G. V. KOKOSH, and S. S. SINANI, *Soviet Phys.-Tech. Phys.* **3** (1958) 1.
12. W. C. MYERS and R. T. BATE, *Bull. Am. Phys. Soc.* **4** (1959) 409.
13. R. J. PRICE, *Phil. Mag.* **46** (1955) 1252.
14. C. Y. LI, A. L. RUOFF, and C. W. SPENCER, *J. Appl. Phys.* **32** (1961) 1733.
15. I. G. AUSTIN, *Proc. Phys. Soc.* **72** (1958) 545.
16. S. V. AIRAPETIANTS and B. A. EFIMOVA, *Soviet Phys.-Tech. Phys.* **3** (1958) 1632.
17. J. BLACK, E. CONWELL, L. SIEGLE, and C. W. SPENCER, *J. Phys. Chem. Solids* **2** (1957) 240.

18. I. TERAMOTO and S. TAKAYANAGI, *J. Phys. Chem. Solids* **19** (1961) 124.
19. W. M. YIM, E. V. FITZKE, and F. D. ROSI, to be published.
20. D. E. STRICKLER, O. F. TUTTLE, H. J. VAN HOOK, and R. ROY, "Phase equilibrium studies on selected systems", Quarterly Prog. Rep. No. 8, Penn. State U.—RCA (1957); see also M. J. SMITH, R. J. KNIGHT, and C. W. SPENCER, *J. Appl. Phys.* **33** (1962) 2186.
21. E. D. DEVIYAMKOVA, A. V. PEMROV, I. A. SMIRNOV, and B. YA. MOIZHES, *Soviet Phys.-Solid State* **2** (1960) 681.
22. E. H. RATCLIFFE, *Glass Technology* **4** (1963) 113.
23. A. AMITH, private communication (1962).
24. J. R. DRABBLE, *Proc. Phys. Soc.* **72** (1958) 380.
25. J. R. DRABBLE, R. D. GROVES, and R. WOLFE, *Proc. Phys. Soc.* **71** (1958) 430.
26. H. J. GOLDSMID, *J. Appl. Phys.* **32** (1961) 2198.
27. D. S. BEERS, G. D. CODY, and B. ABELES, *Proc. Internal Conf. Phys. Semiconductors* (Exeter, England) (1962).
28. E. F. STEIGMEIER and B. ABELES, *Phys. Rev.* **136** (1964) A1149.
29. B. YATES, *J. Electronics and Control* **6** (1959) 26.
30. U. BIRKHOLZ, *Z. Naturf* **13a** (1958) 780.
31. R. O. CARLSON, *J. Phys. Chem. Solids* **13** (1960) 65.
32. B. I. BOLTAKS and N. A. FEDOROVICH, *Soviet Phys.-Solid State* **4** (1962) 400.
33. J. R. DRABBLE and C. H. L. GOODMAN, *J. Phys. Chem. Solids* **5** (1958) 142.
34. H. J. GOLSMID, *Proc. Phys. Soc.* **72** (1958) 17.
35. B. W. HOWLETT, S. M. MISRA, and M. B. BEVER, *Trans. Met. Soc. AIME* **230** (1964) 1367.
36. S. V. AIRAPETIANTS, *Soviet Phys.-Tech. Phys.* **2** (1957) 429.
37. G. J. COSGROVE, J. P. MCHUGH, and W. A. TILLER, *J. Appl. Phys.* **32** (1961) 621.
38. H. J. GOLDSMID, *Proc. Phys. Soc.* **71** (1958) 633.
39. M. L. BELAYAN and H. KH. ABRIKOSOV, *Proce. Acad. Sci. USSR, Phys. Chem. Sect.* **129** (1959) 897.
40. S. V. AIRAPETIANTS, B. A. EFFIMOVA, T. S. STAVITSKAIA, L. S. STIL'BANS, and L. M. SYSOEVA, *Soviet Phys.-Tech. Phys.* **2** (1957) 2009.
41. M. S. CROUTHAMEL, private communication (1964).